Acta Pharmacologica Sinica (2016) 37: 783–793
© 2016 CPS and SIMM All rights reserved 1671-4083/16
www.nature.com/aps

Original Article

Chinese medicine CGA formula ameliorates DMN-induced liver fibrosis in rats via inhibiting MMP2/9, TIMP1/2 and the TGF-β/Smad signaling pathways

Xue-mei LI[1, 6, #], Jing-hua PENG[1, 4, 5, #], Zhao-lin SUN[3], Hua-jie TIAN[1], Xiao-hua DUAN[1], Lin LIU[1], Xin MA[1], Qin FENG[1, 4, 5], Ping LIU[1, 2, 4], Yi-yang HU[1, 2, 4, *]

[1]Institute of Liver diseases, Shuguang Hospital affiliated to Shanghai University of Traditional Chinese Medicine, Shanghai 201203, China; [2]E-Institute of TCM Internal Medicine, Shanghai Municipal Education Commission, Shanghai 201203, China; [3]Shanghai Institute of Materia Medica, Chinese Academy of Sciences, Shanghai 201203, China; [4]Key Laboratory of Liver and Kidney Diseases (Shanghai University of Traditional Chinese Medicine), Ministry of Education, Shanghai 201203, China; [5]Shanghai Key Laboratory of Traditional Chinese Clinical Medicine, Shanghai 201203, China; [6]The First Teaching Hospital of Tianjin University of Traditional Chinese Medicine, Tianjin 300193, China

Aim: Chinese medicine CGA formula consists of polysaccharide from *Cordyceps sinensis* mycelia (CS-PS), gypenosides and amygdalin, which is derived from Fuzheng Huayu (FZHY) capsule for treating liver fibrosis. In this study we attempted to confirm the therapeutic effects of CGA formula in dimethylnitrosamine (DMN)-induced liver fibrosis in rats, and to identify the mechanisms of anti-fibrotic actions.

Methods: Rats were injected with DMN (10 mg·kg^{-1}·d^{-1}, ip) for 3 consecutive days per week over a 4-week period. The rats then were orally administered with CGA formula (CS-PS 60 mg·kg^{-1}·d^{-1}, gypenosides 50 mg·kg^{-1}·d^{-1} and amygdalin 80 mg·kg^{-1}·d^{-1}) daily in the next 2 weeks. CS-PS, gypenosides or amygdalin alone were administered as individual component controls, whereas colchicine and FZHY were used as positive controls. Serum biomarkers were measured. Hepatic injury, collagen deposition and stellate cell activation were examined. The MMP activities, expression of TIMP protein and proteins involved in the TGF-β1/Smad signaling pathways in liver tissues were assayed.

Results: In DMN-treated rats, administration of CGA formula significantly decreased serum ALT, AST and total bilirubin and hepatic hydroxyproline levels, increased serum albumin level, and attenuated liver fibrosis as shown by histological examination. Furthermore, these effects were comparable to those caused by administration of FZHY, and superior to those caused by administration of colchicine or the individual components of CGA formula. Moreover, administration of CGA formula significantly decreased the protein levels of α-SMA, TGF-β1, TGF-β1 receptor (TβR-I), p-TβR-I, p-TβR-II, p-Smad2, p-Smad3, TIMP1 and TIMP2, as well as MMP2 and MMP9 activities in liver tissues of DMN-treated rats.

Conclusion: Chinese medicine CGA formula ameliorates DMN-induced liver fibrosis in rats, and this effect was likely associated with the down-regulation of MMP2/9 activities, TIMP1/2 protein expression and the TGF-β1/Smad signaling pathways in the liver.

Keywords: Chinese medicine; CGA formula; Fuzheng Huayu capsule, liver fibrosis; dimethylnitrosamine; TGF-β1; Smad; MMP2/9; TIMP1/2

Acta Pharmacologica Sinica (2016) 37: 783–793; doi: 10.1038/aps.2016.35; published online 2 May 2016

Introduction

Liver fibrosis is the generic response to chronic injury of varying etiologies, including chronic hepatitis B and C, non-alcoholic fatty liver disease, alcoholic liver disease, drug-induced hepatitis, immune-mediated liver diseases and cholestasis[1]. Hepatic fibrosis ultimately leads to cirrhosis because of the pathological progression, and this is accompanied by severe complications, including liver failure, ascites, portal hypertension, encephalopathy, and hepatocellular carcinoma. Reversing hepatic fibrosis is the key step in blocking pathological progression to cirrhosis[2].

# These authors contributed equally to this work.
* To whom correspondence should be addressed.
E-mail yyhuliver@163.com
Received 2015-10-10 Accepted 2016-01-05

Overproduction and irregular deposition of extracellular matrix (ECM) in liver tissue is the main pathological feature of hepatic fibrosis and leads to distortion of the hepatic microstructure and dysfunction of the liver[3]. Overwhelming evidence supports the idea that activated hepatic stellate cells (HSCs) are the key source of ECM[2]. Transforming growth factor-β (TGF-β) is the most potent of the fibrogenic cytokines, and the TGF-β signaling pathway is a core pathway in HSC activation and hepatic fibrogenesis[4]. In addition to ECM synthesis, the pathological process of liver fibrosis also involves major changes in matrix degradation, which is under the combined regulation of matrix metalloproteinases (MMPs) and tissue inhibitors of metalloproteinases (TIMPs)[5].

The CGA formula consists of polysaccharides from *Cordyceps sinensis* mycelia (CS-PS), gypenosides from *Gynostemma* pentaphyllum and amygdalin from semen persicae (seed of *Prunus persica* (L) Batsch), and it is derived from a traditional Chinese medicine, Fuzheng Huayu (FZHY) capsules. FZHY has been approved and used clinically for the treatment of liver fibrosis caused by hepatitis B in China for decades[6, 7]. FZHY consists of six Chinese medicinal herbs: Radix Salvia Miltiorrhizae (*Salvia miltiorrhiza* root), *Cordyceps sinensis* mycelia, semen persicae, *Gynostemma pentaphyllum*, Pollen Pini (*Pinus thunbergii* pollen), and Fructus Schisandrae Chinensis (*Schisandra chinensis* fruit). Recently, a phase II clinical trial of the anti-fibrotic activity of FZHY in chronic hepatitis C patients with hepatic fibrosis was completed in the US (Trial No NCT00854087), and the subjects who received FZHY exhibited amelioration or stabilization of their liver fibrosis[8]. FZHY is an herbal medicine composed of multiple components, but it is unclear which components are the active anti-fibrotic components. In our previous study of liver fibrosis induced by dimethylnitrosamine (DMN) and carbon tetrachloride (CCl_4) in rats, the primary active components of each Chinese medicinal herb presented in FZHY were screened at different dosages using a uniform design, and hepatic hydroxyproline (Hyp) was used as the screening index[9]. The regression equation indicated that the formula consisting of CS-PS (60 mg/kg per day), gypenosides (50 mg/kg per day) and amygdalin (80 mg/kg per day) was the effective formula, and this was named CGA[9].

CGA has been demonstrated to inhibit HSC activation *in vitro*[10]. The present study sought to confirm the anti-fibrotic activity of CGA and to identify its probable mechanism of action, including its effect on the TGF-β1 signaling pathway, MMP activity and TIMP protein expression. The DMN-induced hepatic fibrosis was induced in rats. CS-PS, gypenosides and amygdalin were used at the previously reported liver-protective doses[11–13] as individual component controls for CGA.

Colchicine is an alkaloid agent that improves clinical laboratory values, decreases fibrosis markers and prolongs survival in patients with mild to moderate cirrhosis[14, 15]. Colchicine and FZHY were used as positive controls in the present study.

Materials and methods

Materials

CS-PS was purchased from Kangzhou Fungi Extract Co, Ltd (Shanghai, China). *Gynostemma pentaphyllammak* gypenosides were purchased from Xi-an Honson Biotechnology Co, Ltd (Xi-an, China). Amygdalin ([(6-O-β-D-glucopyranosyl-β-D-glucopyranosyl)oxy](phenyl)acetonitrile) (Supplementary Figure S1, purity ≥98%) was a commercial product of Shanghai Winherb Medical Technology Co, Ltd (Shanghai, China).

Preliminary chemical analyses of gypenosides and CS-PS

The gypenosides were analyzed using high-pressure liquid chromatography (HPLC). Gypenoside A and gypenoside XLIX (Chengdu Must Biotechnology Co, Ltd, Chengdu, China) were dissolved in 50% acetonitrile and methanol, respectively, and used as the standard. The gypenosides were dissolved in 50% acetonitrile, filtered through 0.2-μm nylon filters and analyzed using HPLC (Agilent 1200 Series, Santa Clara, CA, USA). Chromatographic separation was performed using a mixture of acetonitrile and water, and the mobile phase was as described in Supplementary Table S1. The column eluent was monitored at 250 nm. Chromatography was performed at room temperature with a flow rate of 1.0 mL/min, and a 20-μL sample was analyzed. Analysis demonstrated that the gypenosides contained 18.16% gypenoside XLIX and 44.68% gypenoside A (Supplementary Figure S2).

The total carbohydrate content of CS-PS was determined using the phenol-sulfuric acid method, as described previously[13, 16]. CS-PS (10 mg) was dissolved in 20 mL of deionized water and centrifuged at 1000×*g* for 10 min. The supernatant (3 mL) was removed into a clean tube and diluted to 25 mL with deionized water. Two milliliters of the prepared sample solution of CS-PS was added to the test tube for detection. An aqueous solution of glucose (2 mL, containing glucose 0–48 μg/mL) was used as the standard to obtain the standard curve (Supplementary Figure S3). One milliliter of a 6% phenol solution was added to the standard and experimental tubes and mixed. Concentrated H_2SO_4 (5 mL) was added, and the mixture was vortexed and incubated at room temperature for 30 min (Supplementary Table S2). The absorbance was read three times at 490 nm using an ultraviolet visible spectrophotometer (Shanghai Spectrum Instruments Co, Ltd, Shanghai, China). The total carbohydrate content of CS-PS was 32.2%±0.4% according to the calibration curve (Supplementary Figure S3).

The carbohydrate composition of CS-PS was analyzed using a gas chromatograph-mass spectrometer (GC-MS) (Thermo Fisher Scientific Inc, Waltham, MA, USA). CS-PS (5 mg) was hydrolyzed at 120 °C in 3 mL of 2.0 mol/L trifluoroacetic acid for 2 h. The solution was cooled at room temperature, vacuum dried at 60 °C and dissolved in 2 mL methanol followed by vacuum drying. This process was repeated three times. The residue was reacted with 100 mg sodium borohydride and 2 mL double-distilled water at room temperature, over night. Acetic anhydride (2 mL) was added, and the mixture

was maintained at 100 °C for another 60 min. The sample was analyzed using GC-MS (TRACE-DSQ). Analysis revealed that 100 mg CS-PS contained 0.7±0.01 mg ribose, 0.32±0.04 mg arabinose, 11.0±0.62 mg mannose, 83.71±0.54 mg glucose and 4.27±0.12 mg galactose (Supplementary Figure S4).

Animals and treatment

Male Wistar rats (Experimental Animal Centre, Chinese Academy of Sciences, Shanghai, China; certificate number: SCXK 2007-0005) weighing 150±10 g, SPF grade, were used in this study. The animals were housed in a controlled environment (25 °C, 12 h dark/light cycle). Experiments were performed in accordance with the principles for laboratory animal use and care, and the local ethics committee approved all studies.

Liver fibrosis in rats was induced using intraperitoneal (ip) injections of 10 mg/kg DMN (Tokyo Chemical Industry Co Ltd, Tokyo, Japan) for 3 consecutive days each week over a 4-week period using a method modified from the previous study[17]. Rats in the control group were injected with an equal volume of saline.

Sixty rats were randomly divided into control (n=5) and DMN-stimulated groups (n=55) for dose-effect response testing. After 4 week of DMN stimulation, 16 rats died and the left were then divided into DMN (n=12), DMN plus CGA (CS-PS, 60 mg/kg per day; gypenosides, 50 mg/kg per day; amygdalin, 80 mg/kg per day) (n=9), DMN plus CGA-low dosage (CS-PS, 30 mg/kg per day; gypenosides, 25 mg/kg per day; amygdalin, 40 mg/kg per day) (n=9), and DMN plus FZHY (Pearl Ocean Pharmaceutical Holdings Ltd, Shanghai, China, 4.6 g/kg per day) (n=9) groups.

To observe the effects of CGA on HSC activation, MMPs, TIMPs and TGF-beta1 signaling pathway, eighty-six rats were randomly divided into control (n=6) and DMN-stimulated groups (n=80). After 4 week of DMN stimulation, 18 rats died and the left were then divided into: DMN (n=9), DMN plus CS-PS (Kangzhou Fungi Extract Co, Ltd, Shanghai, China, 60 mg/kg per day) (n=9), DMN plus gypenosides (Xi-an Honson biotechnology Co, Ltd, Xi-an, China, 200 mg/kg per day) (n=9), DMN plus amygdalin (Xi-an Guanyu Biotechnology Co Ltd, Xi-an, China, 80 mg/kg per day) (n=9), DMN plus CGA (CS-PS, 60 mg/kg per day; gypenosides, 50 mg/kg per day; amygdalin, 80 mg/kg per day) (n=8), DMN plus FZHY (Pearl Ocean Pharmaceutical Holdings Ltd, Shanghai, China, 4.6 g/kg per day) (n=9) and DMN plus colchicine (Kunming Pharmaceutical Corp, Kunming, China, 0.1 mg/kg per day) (n=9). Drugs were dissolved in double-distilled water (DDW) and administered via intragastric gavage (ig) daily. Rats in the control and DMN groups received an equal volume of DDW ig.

Drugs were orally administered during the last 2 week, and rats were then anesthetized with nembutal (45 mg/kg, ip). Serum and liver tissue were sampled and stored at -80 °C for analysis.

Histological examinations

Liver tissue was fixed in formalin and embedded in paraffin. Specimens (4 μm) were stained with hematoxylin-eosin (H&E, Nanjing Jiancheng Bioengineering Institute, Nanjing, China) and observed under a light microscope (Olympus Medical Systems Corp, Tokyo, Japan).

Liver sections (5 μm) were stained with Sirius red for collagen deposition. A previously described grading system for fibrosis and cirrhosis[18] (Table 1) was used to identify the stage of hepatic pathological changes.

Table 1. Hepatic fibrosis grading system.

Grade	Fibrosis
0	None
I	Enlarged, fibrotic portal tracts
II	Periportal or portal-portal septa but intact architecture
III	Fibrosis with architectural distortion but no obvious cirrhosis
IV	Probable or definite cirrhosis

Serum ALT, AST, Alb, TBil and hepatic Hyp assays

Serum alanine aminotransferase (ALT), aspartate aminotransferase (AST), albumin (Alb) and total bilirubin (TBil) levels were measured using the corresponding biochemical assay kits (Nanjing Jiancheng Bioengineering Institute, Nanjing, China). Hepatic Hyp content was examined using the previously reported method with slight modifications[19]. Briefly, 100 mg of liver tissue was homogenized and dissolved in 5 mL of 6 mol/L HCL at 110 °C for 18 h. The hydrolysate was filtered through a Millipore filter (0.45 μm, Millipore, Darmstadt, Germany), and 100 μL was removed to a clean tube and dried at 40 °C. The specimens were incubated with Ehrlich's reagent (25% [w/v] para-dimethylaminobenzaldehyde and 27.3% [v/v] perchloric acid in isopropanol) at 50 °C for 90 min and cooled to room temperature. The optical density of the samples was read at 558 nm (SpectraMax M5; Molecular Devices, Sunnyvale, CA, USA) against a reagent blank, and the Hyp content was determined from the Hyp standard curve (Nakateyitesuku Company, Japan). Hyp results are presented as mg per g liver tissue.

Immunohistochemical analysis of hepatic α-SMA

Paraffin-embedded slices (4 μm) were used for immunohistochemical assessment using a method described in a previous study[20]. Briefly, endogenous peroxidase was blocked with 0.3% H_2O_2, and non-specific binding sites were blocked with bovine serum albumin. The samples were incubated with a smooth muscle actin (α-SMA)-specific antibody (1:400 dilution, Mouse IgG2a α-SMA; Sigma, MO, USA) at 4 °C overnight, followed by incubation with a 1:250 dilution of a horseradish peroxidase (HRP)-linked goat anti-mouse IgG (Santa Cruz Biotechnology Inc, Santa Cruz, CA, USA) for 1 h at 37 °C. Diaminobenzidine (DAB) was used as a chromogen, and hematoxylin was used for nuclear staining.

Sections were scanned using a Leica SCN400 scanning system (Leica Biosystems Inc, Buffalo Grove, IL, USA), and all

images were analyzed using Image Pro Plus software (Media Cybernetics, Inc, Rockville, MD, USA). The integrated optical density of five high-power fields (×400 magnification) of each section was calculated and corrected for the area of each section stained.

Western blot analysis

The protein expression of α-SMA, TGF-β1, TGF-β1 receptor I (TβR-I), TGF-β1 receptor II (TβR-II), phosphorylated TGF-β1 receptor (p-TβR)-I, p-TβR-II, Smad2/3, phosphorylated Smad2/3 (p-Smad2/3), TIMP1 and TIMP2 in liver tissue were detected using Western blot analysis, as described previously[20]. The total protein concentrations of liver tissue extracts were determined using a bicinchoninic acid (BCA) protein concentration assay kit (Beyotime Biotechnology, Haimen, China). A 10% SDS-PAGE separating gel and Bio-Rad electrophoresis system (BioRad Laboratories, Hercules, CA, USA) were used to separate proteins. Blots were incubated with primary antibodies (Table 2) at 4 °C overnight and then the corresponding HRP-conjugated secondary antibodies at room temperature for 1 h. An enhanced chemiluminescence kit (Pierce Biotechnology Inc, Rockford, IL, USA) and the Furi FR-980 image analysis system (Shanghai Furi Co, Shanghai, China) were used for chemiluminescence detection. The GAPDH protein was used as the internal control.

Gelatin zymography

MMP2 and MMP9 activity were assessed using gelatin zymography as previously described[19, 21]. Total protein was extracted with the addition of RIPA solution (containing 1 mol/L Tris–HCl and 0.5 mol/L NaCl, pH 7.0) and separated using electrophoresis in 0.1% gelatin and an 8% stacking gel at 4 °C, followed by elution with elution buffer (containing 2.5% Triton X-100, 50 mmol/L Tris–HCl, 5 mmol/L $CaCl_2$, and 1 mmol/L $ZnCl_2$, pH 7.6) for 45 min, twice. Gels were rinsed twice (rinsing buffer containing 50 mmol/L Tris–HCl, 5 mmol/L $CaCl_2$, and 1 mmol/L $ZnCl_2$, pH 7.6) for 30 min. Gels were then incubated in buffer (containing 50 mmol/L Tris–HCl, 5 mmol/L $CaCl_2$, 1 mmol/L $ZnCl_2$, and 0.02% Brij-35, pH 7.6) on incubating shakers at 37 °C for 18 h, stained with a mixture of 0.05% Coomassie blue G-250 R-250, 30% methanol and 10% acetic acid for 3 h, and then destained in solution A (containing 30% methanol and 10% acetic acid), solution B (containing 20% methanol and 10% acetic acid) and solution C (containing 10% methanol and 5% acetic acid). The Furi FR-980 image analysis system (Shanghai Furi Co, Shanghai, China) was used to assess band intensity.

Statistical analysis

Data are presented as the mean±SD. The statistical significance of the differences was analyzed using one-way analysis of variance (ANOVA), followed by the least significant difference (LSD) *post hoc* test. The *t*-test was used for comparisons between two parameters. Fibrosis grading was analyzed using ridit analysis. Differences were considered statistically significant when $P<0.05$.

Results

Dose-effect response of CGA on DMN-induced liver fibrosis

Sixteen rats in the DMN-stimulated group died in the first four weeks of the dose-effect response test. Five rats died in the DMN group in the subsequent two weeks of treatment; one rat died in the DMN plus CGA group, and two rats in the DMN plus CGA-low dosage and DMN plus FZHY groups died.

Dose-dependent effects of CGA were observed on liver fibrosis in DMN-stimulated rats. The effects of CGA on hepatic Hyp concentration (Supplementary Table S3), serum ALT, AST, Alb (Supplementary Table S4), and fibrosis grading in the liver (Supplementary Table S5) were all superior to that of low-dose CGA. Therefore, CGA composed of CS-PS (60 mg/kg per day), gypenosides (50 mg/kg per day) and amygdalin (80 mg/kg per day) was used in the subsequent

Table 2. Antibodies in immunohistochemical assay and immunoblot.

Antibody	Species	Brand	Dilution
α-SMA	Mouse IgG2a	Sigma, MO, USA	1:400
TIMP-1	Mouse IgG1	Lab Vision, USA	2 μg/mL
TIMP-2	Mouse IgG1	Lab Vision, USA	2 μg/mL
TGF-β1	Mouse IgG1	Abcam, UK	1:2000
TbR-I	Rabbit IgG	Cell Signaling, MA, USA	1:1000
TbR-II	Rabbit IgG	Cell Signaling, MA, USA	1:1000
p-TβR I	Rabbit IgG	Signalway Antibody LLC, MD, USA	1:1000
p-TβR II	Goat IgG	Cell Signaling, MA, USA	1:200
Smad2	Mouse IgG1	Cell Signaling, MA, USA	1:1000
Smad3	Rabbit IgG1	Cell Signaling, MA, USA	1:1000
p-Smad2	Rabbit IgG	Abcam, UK	1:300
p-Smad3	Rabbit IgG	Epitomics, CA, USA	1:1000
GAPDH	Mouse IgG1	Kangchen, Shanghai, China	1:5000
HRP-linked antibody	Goat anti rabbit IgG	Santa Cruz, CA, USA	1:5000
HRP-linked antibody	Goat anti mouse IgG	Santa Cruz, CA, USA	1:5000

experiments.

Mortality, body weight and liver/spleen weight ratio

Eighteen rats in the DMN-stimulated group died in the first four weeks. One rat died in the DMN, DMN plus gypenosides, DMN plus amygdalin and DMN plus colchicine groups in the subsequent two weeks. Two rats died in the DMN plus CS-PS and DMN plus FZHY groups. No rats died in the control group or the DMN plus CGA group.

The body weight and the liver/spleen weight ratio decreased in the DMN group compared to the control (P<0.01). There was no significant change in body weight in the drug-treated groups compared with the DMN group. However, CGA, CS-PS, gypenosides, amygdalin or FZHY treatment significantly increased the liver/spleen weight ratio compared to the DMN group (Table 3).

Table 3. Body weight and the liver/spleen weight ratio of rats.

Group	*n*	Body weight (g)	Liver/spleen weight ratio
Control	6	375±12	13.04±1.12
DMN	8	272±29**	4.03±1.51**
CS-PS	7	267±41	6.29±2.75$^{\#}$
Gypenosides	8	269±36	6.25±1.86$^{\#}$
Amygdalin	8	277±33	6.11±2.30$^{\#}$
CGA	8	285±32	6.35±1.22$^{\#\#}$
FZHY	7	292±40	6.87±0.59$^{\#\#}$
Colchicine	8	280±43	5.30±3.20

Data represent mean±standard deviation. $^{**}P$<0.01 *vs* control group; $^{\#}P$<0.05, $^{\#\#}P$<0.01 *vs* DMN group.

Effects of CGA formula on DMN-induced liver injury

DMN-induced liver injury was assayed using serum biomarkers and histological changes in liver tissue. H&E staining revealed typical pseudo lobules, a large amount of fibrous connective tissue, hepatocyte swelling, and inflammatory cell infiltration following DMN administration. Fewer complete pseudolobules, thinner fibrous connective tissue and recovered sinusoids were observed in the CGA and FZHY treatment groups. The hepatic pathological changes in the other treatment groups were also ameliorated to some degree. However, some pseudolobules were visualized in the colchicine-treated group (Figure 1A).

Serum ALT (P<0.01), AST (P<0.01) and TBil (P<0.01) levels increased significantly and the Alb level decreased (P<0.01) significantly with DMN stimulation. Serum ALT (P<0.01), AST (P<0.01), and TBil (P<0.01) levels decreased and the Alb level increased (P<0.05) in the CGA treatment group compared to the DMN group, and the effects were comparable to those in FZHY-treated rats (P>0.05). In contrast, the inhibitory effect of CGA on ALT was superior to that of amygdalin (P<0.05), and the inhibitory effect of CGA on TBil was superior to that of CS-PS (P<0.01) and gypenosides (P<0.05). Serum Alb level did not increase with colchicine (P>0.05) or amygdalin (P>0.05) treatment compared with that in the DMN group (Figure 1C).

Effects of CGA formula on collagen deposition in DMN-stimulated liver tissue

DMN administration induced collagen deposition in liver tissue, especially in the peri-sinusoidal areas, in Sirius red stained sections, and numerous complete pseudolobules and fibrous septa were also observed between the portal area and central venous area (Figure 1B). Collagen deposition was obviously ameliorated in the CGA or FZHY-treated groups compared to the DMN group, and few complete pseudolobules were observed. The collagen staining with Sirius red was weaker with colchicine, CS-PS, gypenosides or amygdalin treatment compared to that of the DMN group, but some pseudolobules were visible in the colchicine group (Figure 1B). Fibrosis grading based on the Sirius red staining data also showed that a much higher fibrosis score was obtained in the DMN-stimulated group than in the control or CGA (P<0.01), FZHY (P<0.01) or colchicine (P<0.05) treatment groups. Fibrosis grading also decreased compared to the DMN group (Figure 1C).

The hepatic Hyp content of rats in the DMN group obviously increased compared to the control (P<0.01). Hyp content decreased dramatically with CGA treatment (P<0.01), and this decrease was comparable to that in the FZHY (P>0.05) group and superior to that in the colchicine (P<0.05), CS-PS (P<0.05), gypenoside (P<0.05) and amygdalin (P<0.05) treatment groups (Figure 1C).

Effect of CGA formula on hepatic α-SMA expression

HSC activation is characterized by proliferation and myofibroblastic transformation. α-SMA is a marker of activated HSCs, which show a myofibroblastic phenotype[22].

The expression of α-SMA protein in liver tissue increased markedly (P<0.01) with DMN administration and decreased dramatically with CGA (P<0.01), FZHY (P<0.01), CS-PS (P<0.01) or gypenoside (P<0.05) treatment. However, α-SMA was not altered in amygdalin- or colchicine-treated groups (Figure 2A and 2B).

Similarly, positive α-SMA staining was observed only in vessel walls in the control group, but much stronger positive α-SMA staining was found on fibrous septa in the DMN group. Weaker staining was observed in the CGA-, FZHY-, CS-PS- and gypenoside-treated groups. However, positive α-SMA staining was not obviously weaker in the amygdalin and colchicine-treated groups than in the DMN group (Figure 2C). Semi-quantitation of α-SMA immunohistochemical staining indicated that the relative optical density of the α-SMA positive area increased with DMN stimulation (P<0.01) and clearly decreased in the CS-PS, gypenoside, CGA, FZHY and colchicine treatment groups (P<0.01, Supplementary Figure S5).

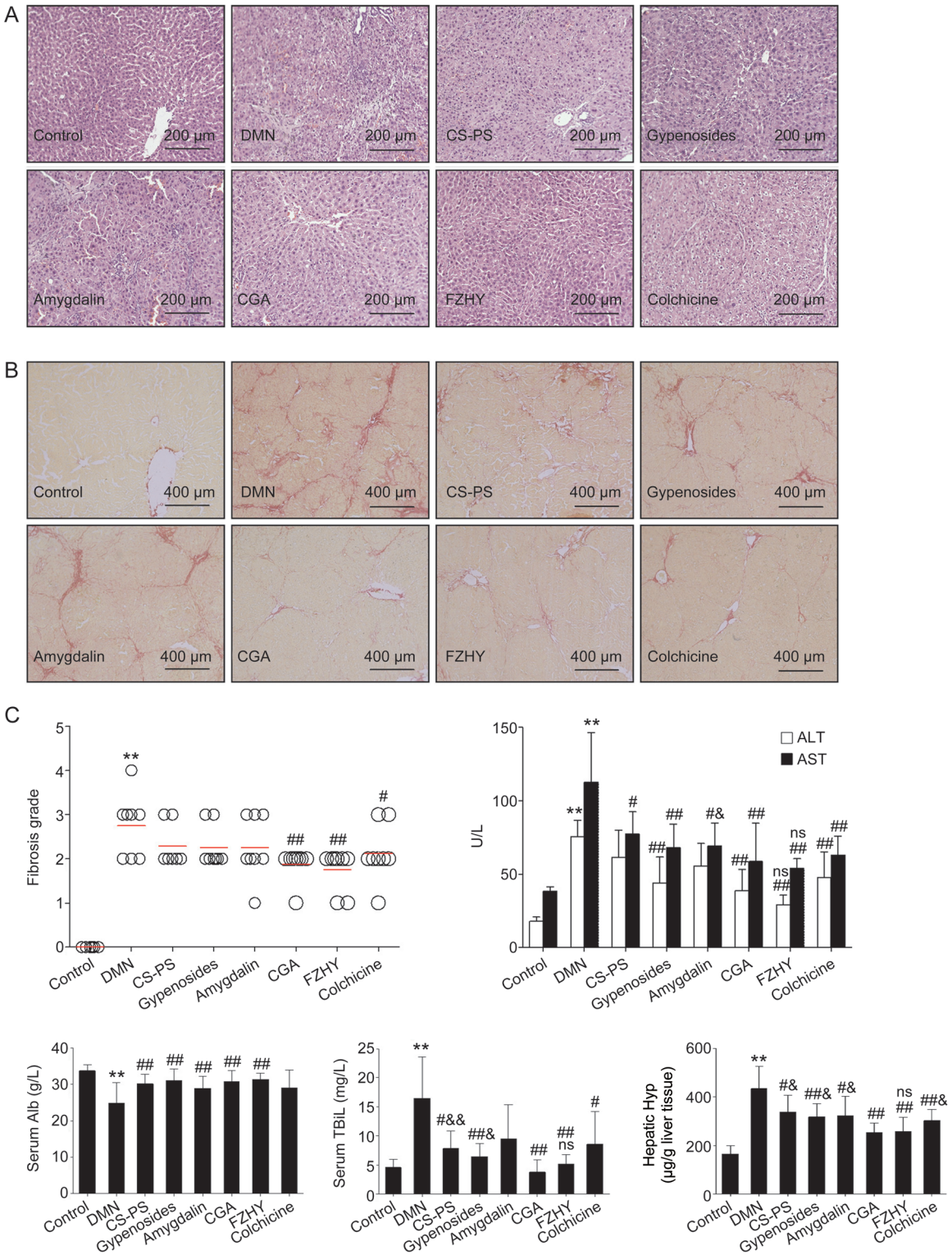

Figure 1. Effects of CGA on liver injury and collagen deposition. (A) Histological changes visualized in hematoxylin and eosin (H&E) staining, original magnification ×200. With dimethylnitrosamine (DMN) stimulation, typical pseudo lobules and large amounts of fibrous connective tissue were observed, as well as hepatocytes swelling, inflammatory cells infiltration. In the CGA and FZHY treatment group, fewer complete pseudo lobules, thinner fibrous connective tissue were observed. (B) Collagen deposition visualized in Sirius red staining, original magnification ×100. With DMN administration, hepatic collagen deposition was obvious and numerous complement pseudo lobules were observed. Few pseudo lobules and collagen deposition was found in the CGA and FZHY treatment group. (C) Fibrosis grading based on Sirius red staining, serum Alanine aminotransferase (ALT), aspartate aminotransferase (AST), albumin (Alb), total bilirubin (TBiL) and hepatic hydroxyproline (Hyp) content. Data represents mean±standard deviation ($n \geq 6$). $^{**}P<0.01$ *vs* control; $^{\#}P<0.05$, $^{\#\#}P<0.01$ *vs* DMN; $^{ns}P>0.05$, $^{\&}P<0.05$, $^{\&\&}P<0.01$ *vs* DMN+CGA.

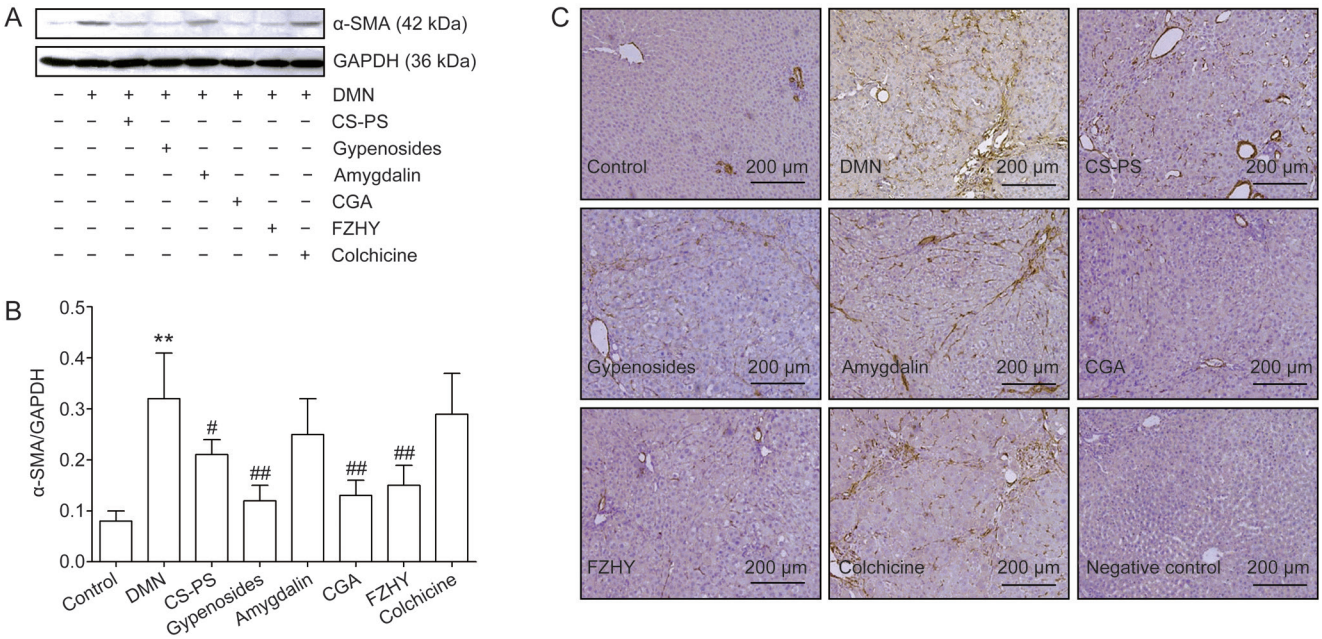

Figure 2. Effects of CGA on α-smooth muscle actin (α-SMA) expression in liver tissue. (A) Protein expression of α-SMA in liver tissue detected by Western-blot analysis. (B) Band intensity of α-SMA was normalized to GAPDH and expressed as α-SMA/GAPDH ratio. α-SMA protein expression increased remarkably with DMN administration and decreased dramatically with CGA, FZHY, CS-PS and gypenosides treatment. Data represent mean±standard deviation. All experiments were performed in different samples independently in triplicate. $^{**}P<0.01$ *vs* control; $^{\#}P<0.05$, $^{\#\#}P<0.01$ *vs* DMN. (C) Protein expression of α-SMA in liver tissue detected by immunohistology, original magnification ×200. In control group, the positive α-SMA staining was only observed in vessel wall. Much stronger positive staining of α-SMA was found located on the fibrous septa in DMN group, which was light colored in CGA, FZHY, CS-PS and gypenosides-treated groups.

Effects of CGA formula on TGF-β1, TβR-I, TβR-II, p-TβR-I, p-TβR-II protein expression

TGF-β1 signaling is dependent on TβR-I, TβR-II and the down-stream phosphorylation of Smad proteins. TGF-β1 binding to TβR-II leads to the formation and stabilization of a TβR-I/TβR-II complex. Then, TβR-I is phosphorylated, and TβR-II kinase activates Smad2 and Smad3. Phosphorylated Smad2 and Smad3 then form a complex that translocates to the nucleus and serves as a transcriptional regulator[23]. Six weeks of DMN administration increased the protein level of TGF-β1 ($P<0.05$), TβR I ($P<0.01$) and p-TβR-I ($P<0.01$) in liver tissue. CGA or FZHY treatment decreased the TGF-β1 protein level ($P<0.05$, treated with CGA; $P<0.05$, treated with FZHY), TβR-I protein level ($P<0.05$, treated with CGA; $P<0.01$, treated with FZHY) and p-TβR-I protein level ($P<0.05$, treated with CGA; $P<0.01$, treated with FZHY). Colchicine treatment inhibited DMN-induced protein expression of TβR-I ($P<0.05$) but not TGF-β1 or p-TβR-I. Individual component treatment also altered the protein levels of TGF-β1, TβR-I and p-TβR-I in the liver: TGF-β1 ($P<0.05$), TβR-I ($P<0.01$) and p-TβR-I ($P<0.05$) levels were lower in the gypenoside-treated group, and TβR-I and p-TβR-I levels were lower in the CS-PS-treated group ($P<0.01$). In contrast, DMN administration did not obviously alter TβR-II protein expression, but the p-TβR II protein level increased with DMN stimulation and decreased in the CGA group ($P<0.01$, Figure 3).

Effects of CGA formula on Smad2/p-Smad2 and Smad3/p-Smad3 protein levels

The protein levels of p-Smad2 ($P<0.01$) and p-Smad3 ($P<0.01$) increased with DMN administration and decreased with CGA ($P<0.01$, on p-Smad2; $P<0.05$, on p-Smad3), FZHY ($P<0.01$, on p-Smad2; $P<0.05$, on p-Smad3), CS-PS ($P<0.01$, on p-Smad2; $P<0.05$, on p-Smad3) or gypenoside ($P<0.05$, on p-Smad2; $P<0.05$, on p-Smad3) treatment. Colchicine decreased the protein level of p-Smad 3 ($P<0.05$) but not p-Smad 2. In contrast, there were no obvious changes in the protein expression of Smad-2 and Smad-3 in liver tissue (Figure 4).

Effects of CGA formula on MMP2 and MMP9 activity and protein expression of TIMP-1 and TIMP-2

The expression of TIMP-1 ($P<0.01$) and TIMP-2 ($P<0.01$) protein in liver tissue was increased with DMN administration and decreased in the CGA ($P<0.05$, on TIMP1; $P<0.05$, on TIMP2), FZHY ($P<0.01$, on TIMP1; $P<0.05$, on TIMP2) and colchicine ($P<0.01$, on TIMP1; $P<0.05$, on TIMP2) groups (Figure 5A and 5B). Similarly, MMP2 ($P<0.01$) and MMP9 ($P<0.01$) activity in liver tissue was increased following six weeks of DMN administration and decreased only in the CGA ($P<0.01$, on MMP2; $P<0.01$, on MMP9) or FZHY groups ($P<0.01$, on MMP2; $P<0.05$, on MMP9) (Figure 5A and 5C).

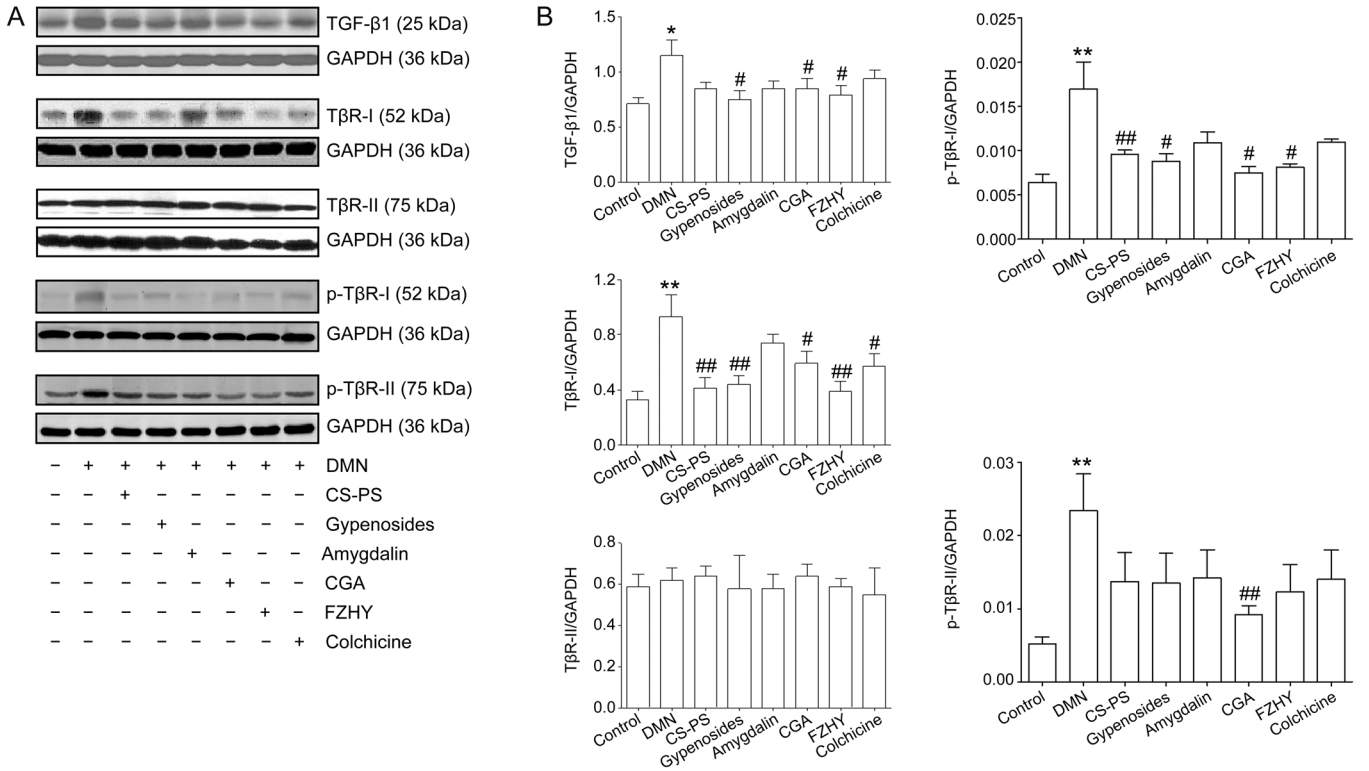

Figure 3. Effects of CGA on the protein expression of transforming growth factor-β1 (TGF-β1), TGF-β1 receptor (TβR)-I, phosphorylated TGF-β1 receptor (p-TβR)-I, TβR-II and p-TβR-II in hepatic fibrosis in rat induced by DMN. (A) The protein expression of TGF-β1, TβR-I, p-TβR-I, TβR-II and p-TβR-II in liver tissue detected by Western-blot. (B) Band intensity of TGF-β1, TβR-I p-TβR-I, TβR-II and p-TβR-II was normalized to GAPDH and expressed as fold of GAPDH. Hepatic TGF-β1, TβR-I and p-TβR-I protein was up-regulated with DMN stimulation, and down-regulated in CGA, FZHY and gypenosides groups. TβR-I and p-TβR-I protein expression also decreased in CS-PS group and moreover, TβR-I protein was decreased in colchicine group. No obvious change was detected in hepatic TβR-II protein expression, while the protein expression of p-TβR-II was up-regulated with DMN administration and down-regulated in CGA group. Data represent mean±standard deviation. All experiments were performed in different samples independently in triplicate. $^{*}P<0.05$, $^{**}P<0.01$ *vs* control; $^{\#}P<0.05$, $^{\#\#}P<0.01$ *vs* DMN.

Discussion

DMN-induced liver fibrosis is a classic stable model of fibrosis that progresses for weeks or months after discontinuation of toxin administration[24]. The effects of CGA on serum markers of liver function and histological changes in the present study demonstrated that the effects of CGA on DMN-induced liver injury were comparable to those of FZHY, from which CGA was derived, and these effects were superior at ameliorating the injury to colchicine or the individual components of CGA. Collagen deposition in the liver was demonstrated using Sirius red staining and fibrosis grading, and collagen and hepatic Hyp content revealed that CGA has comparable inhibitory effects to FZHY and superior effects to colchicine or the individual CGA components on DMN-induced liver fibrosis.

HSC activation is a crucial event in liver fibrogenesis[25-27], and it can be divided into initiation and perpetuation[27]. Initiation refers to early changes in gene expression that result primarily from paracrine stimuli derived from damaged resident liver cells (hepatocytes, endothelial cells and Kupffer cells) and platelets[28, 29]. Persistence of the initiation stimuli and the accompanying sustained injury lead to a perpetuation phase, in which at least seven distinct changes in HSC behavior are involved, including proliferation, chemotaxis, fibrogenesis, contractility, matrix degradation alterations, retinoid loss and inflammatory signaling[30]. Increased fibrogenesis is the most direct path by which HSCs contribute to hepatic fibrosis. HSC activation in the present study was inhibited by CGA treatment, and this inhibition was accompanied by the amelioration of hepatic fibrosis.

TGF-β1 is one of the most prominent drivers of cellular activation and the HSC to myofibroblast transdifferentiation[31]. CGA treatment down-regulated TGF-β1 protein expression in DMN-stimulated liver tissue. There are multiple cellular sources of TGF-β1, including Kupffer cells[29], endothelial cells and platelets[28], but HSC autocrine expression is one of the most important sources[32, 33]. *In vitro* primary HSC studies[10] suggest that CGA down-regulated the gene expression of TGF-β1 and TβR in primary HSCs and simultaneously inhibited HSC activation. Therefore, we conclude that activated HSCs are one of the cellular targets of CGA that lead to the inhibition of TGF-β1.

TGF-β signaling is initiated by ligand binding to and complex formation of type I and type II receptor serine/threonine kinases on the cell surface. The formation of this complex

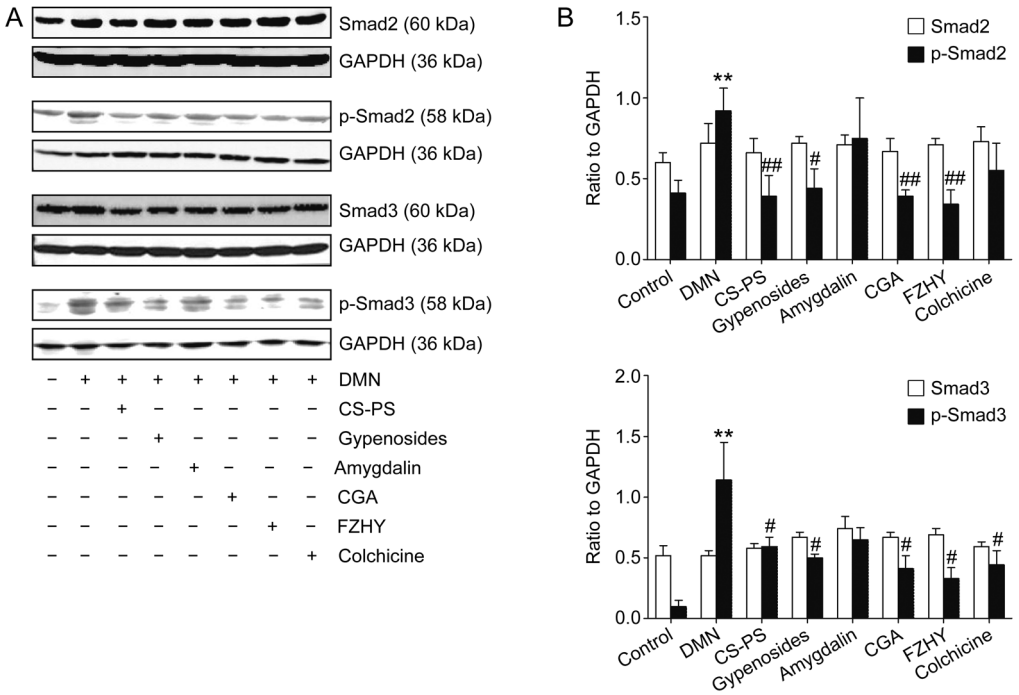

Figure 4. Effects of CGA on Smad2, p-Smad2, Smad3 and p-Smad3 protein expression in hepatic fibrosis in rat induced by DMN. (A) The protein expression of Smad2, p-Smad2, Smad3 and p-Smad3 in liver tissue detected by Western-blot. (B) Band intensity of Smad2, p-Smad2, Smad3 and p-Smad3 was normalized to GAPDH and expressed as fold of GAPDH. Hepatic p-Smad2 and p-Smad3 protein expression was up-regulated with DMN administration and down-regulated with CGA, FZHY, CS-PS and gypenosides treatment. Colchicine down regulated the protein expression of p-Smad3 but not p-Smad2. No obvious changes in the protein expression of Smad2 and Smad3 in the liver tissue. Data represent mean±standard deviation. All experiments were performed in different samples independently in triplicate. $^{**}P<0.01$ *vs* control; $^{\#}P<0.05$, $^{\#\#}P<0.01$ *vs* DMN.

allows the type II receptor to phosphorylate the kinase domain of the type I receptor, which propagates the signal through the phosphorylation of Smad proteins[34]. The levels of TGF-β1, TβRI, p-TβRI, p-TβRII, p-Smad2 and p-Smad3, but not TβRII, proteins were increased significantly in DMN-induced fibrotic liver tissue, and the CGA formula or FZHY treatment markedly decreased the levels of these proteins. These data indicate that the amelioration of liver fibrosis by CGA treatment is likely associated with inhibition of the TGF-β signaling pathway.

TGF-β is synthesized as a prohormone and cleaved in the Golgi to an amino terminal latency-associated protein and a mature TGF-β fragment. These two fragments remain bound to various latent TGF-β binding proteins, which are secreted as a latent complex. Latent TGF-β is activated via multiple mechanisms, including through MMP2 and MMP9[35]. CGA treatment down-regulated MMP2 and MMP9 activity and TGF-β1 protein expression in the present study compared to that in the DMN group, which suggests that the effect of CGA on MMP2 and MMP9 also contributed to the inhibition of TGF-β1. The target cellular source of TGF-β1, the mechanism of CGA inhibition of TGF-β1 and the direct contribution of TGF-β1 to the pharmacological effects of CGA require further investigation.

MMPs and TIMPs closely regulate the degradation and accumulation of the ECM. MMP2 and MMP9 are the most relevant MMPs that degrade normal liver matrix, and these enzymes contribute to the pathogenesis of liver fibrosis, particularly in early responses to liver injury[5]. TIMP1 and TIMP2 inhibit the active forms of MMPs, which cleave types I and III collagen. MMP2 and MMP9 activity and the protein expression of TIMP1 and TIMP2 increased dramatically with DMN administration in the present study and clearly decreased after CGA treatment. These results suggest that the regulation of MMPs and TIMPs by CGA also contributes to the effects of CGA on liver fibrosis.

Fibrosis and cirrhosis are major causes of morbidity and mortality worldwide[1]. Several clinical trials on liver fibrosis are ongoing, but the outcomes of completed trials have not been satisfactory[1]. FZHY is the only herbal medicine that is approved for phase II clinical trials in chronic hepatitis C patients with hepatic fibrosis in the US, and FZHY is safe, well tolerated and tends to stabilize and ameliorate liver fibrosis in chronic hepatitis C patients with moderate to severe fibrosis[8]. CGA is the active component of FZHY and was found to inhibits DMN-induced liver fibrosis in rats in the present research, thereby confirming the anti-fibrotic effect of CGA formula that was uncoveredusing a uniform design in our previous study[9]. The pharmacological effects of CGA formula in the present study were comparable to those of FZHY and superior to those of colchicine and the individual components of CGA. Furthermore, the inhibitory effect of CGA formula

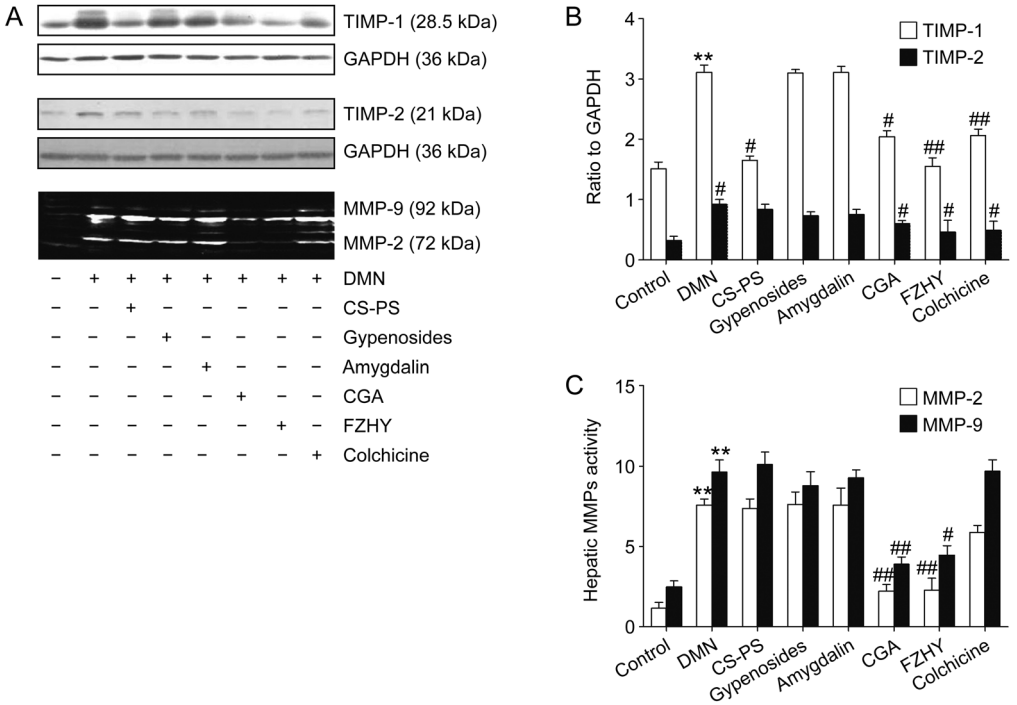

Figure 5. Effcts of CGA on the protein expression of tissue inhibitor of metalloproteinases (TIMP-1/TIMP-2) and the activity of matrix metalloproteinases (MMP-2/MMP-9) in hepatic fibrosis induced by DMN in rats. (A) The protein expression of TIMP-1 and TIMP-2 in liver tissue detected by Western-blot and the activity of MMP-2 and MMP-9 detected by gelatin zymography. (B) Band intensity of TIMP-1 and TIMP-2 was normalized to GAPDH and expressed as fold of GAPDH. The protein expression of TIMP-1 and TIMP-2 in liver tissue increased with DMN administration and decreased in CGA, FZHY and colchicine groups. (C) Band intensity of the activities of MMP-2 and MMP-9 in liver tissue. The activities of MMP-2 and MMP-9 in liver tissue increased remarkably with DMN administration for six weeks and decreased only in CGA and FZHY group. Data represent mean±standard deviation. All experiments were performed in different samples independently in triplicate. $^{**}P<0.01$ *vs* control; $^{\#}P<0.05$, $^{\#\#}P<0.01$ *vs* DMN.

on DMN-induced liver fibrosis was associated with the inhibition of the TGF-β1/Smad signaling pathway and MMPs and TIMPs.

In contrast to FZHY, which consists of six kinds of traditional Chinese herbal medicines, CGA consists of only three herbal components. However, the effects of CGA on liver fibrosis were comparable to those of FZHY. The effects and mechanisms of action of CGA on liver fibrosis deserve further investigation because the effect can be achieved with a smaller dose, quality control is easier and less of the herbal medicine source is needed than with FZYH.

Acknowledgements

This work was supported by the National Science and Technology Major Project of China (2012ZX09103-201-048); the National Natural Science Foundation of China (No 81303071); and the Shanghai Municipal Commission of Health and Family Planning (ZY3-RCPY-2-2010).

Author contribution

Xue-mei LI conducted the experiments and analyzed the data; Jing-hua PENG analyzed and integrated the data and wrote and revised the manuscript; Zhao-lin SUN conducted the chemical analyses of *Cordyceps sinensis* mycelia polysaccharide and *Gynostemma pentaphyllum* gypenosides; Hua-jie TIAN integrated the figures and references and conducted the supplemental experiments during revision; Xiao-hua DUAN conducted the CGA dose-effect response experiments; Lin LIU and Xin MA modified the statements in the "Methods" section; Qin FENG and Ping LIU provided advice during the experiments; and Yi-yang HU designed the study.

Supplementary information

Supplementary information is available at the Acta Pharmacologica Sinica's website.

References

1 Cohen-Naftaly M, Friedman SL. Current status of novel antifibrotic therapies in patients with chronic liver disease. Therap Adv Gastroenterol 2011; 4: 391–417.
2 Lee YA, Wallace MC, Friedman SL. Pathobiology of liver fibrosis: a translational success story. Gut 2015; 64: 830–41.
3 Friedman SL. Liver fibrosis — from bench to bedside. J Hepatol 2003; 38: S38–53.
4 Wallace MC, Friedman SL, Mann DA. Emerging and disease-specific mechanisms of hepatic stellate cell activation. Semin Liver Dis 2015; 35: 107–18.
5 Arthur MJ. Fibrogenesis II. Metalloproteinases and their inhibitors in liver fibrosis. Am J Physiol Gastrointest Liver Physiol 2000; 279: G245–9.
6 Liu C, Hu Y, Xu L, Liu P. Effect of Fuzheng Huayu formula and its

actions against liver fibrosis. Chin Med 2009; 4: 12.
7 Liu P, Hu YY, Liu C, Xu LM, Liu CH, Sun KW, *et al.* Multicenter clinical study on Fuzhenghuayu capsule against liver fibrosis due to chronic hepatitis B. World J Gastroenterol 2005; 11: 2892–9.
8 Hassanein T, Box TD, Tong MJ, Pozza R, Lorenzo O, Jeffrey G, *et al.* A Phase II, randomized, placebo-controlled, double-blind, multi-center study to assess the antifibrotic activity of Fuzheng Huayu in chronic hepatitis C patients with hepatic fibrosis. Gastroenterology 2014; 146: S261.
9 Li XM, Hu YY, Duan XH. Uniform designed research on the active ingredients assembling of Chinese medicine prescription for anti-liver fibrosis. Zhongguo Zhong Xi Yi Jie He Za Zhi 2010; 30: 58–63.
10 Chen L, Feng Q, Peng JH, Liu L, Liang CG, Hai YM, *et al.* Effect of CKJ recipe containing serum on activation of rat primary hepatic stellate cells, TGF-beta1 and its receptors. Zhongguo Zhong Xi Yi Jie He Za Zhi 2015; 35: 210–5.
11 Chen JC, Tsai CC, Chen LD, Chen HH, Wang WC. Therapeutic effect of gypenoside on chronic liver injury and fibrosis induced by CCl_4 in rats. Am J Chin Med 2000; 28: 175–85.
12 Zhou JH, Yumo W, editors. Chinese Medicine Pharmacology. Shanghai Science and Technology Publishing House, Shanghai, China; 1986.
13 Peng J, Li X, Feng Q, Chen L, Xu L, Hu Y. Anti-fibrotic effect of Cordyceps sinensis polysaccharide: Inhibiting HSC activation, TGF-beta1/Smad signalling, MMPs and TIMPs. Exp Biol Med (Maywood) 2013; 238: 668–77.
14 Bodenheimer H Jr, Schaffner F, Pezzullo J. Evaluation of colchicine therapy in primary biliary cirrhosis. Gastroenterology 1988; 95: 124–9.
15 Kershenobich D, Vargas F, Garcia-Tsao G, Perez Tamayo R, Gent M, Rojkind M. Colchicine in the treatment of cirrhosis of the liver. N Engl J Med 1988; 318: 1709–13.
16 Saha SK, Brewer CF. Determination of the concentrations of oligosaccharides, complex type carbohydrates, and glycoproteins using the phenol-sulfuric acid method. Carbohydr Res 1994; 254: 157–67.
17 Ala-Kokko L, Pihlajaniemi T, Myers JC, Kivirikko KI, Savolainen ER. Gene expression of type I, III and IV collagens in hepatic fibrosis induced by dimethylnitrosamine in the rat. Biochem J 1987; 244: 75–9.
18 Scheuer PJ. Classification of chronic viral hepatitis: a need for reassessment. J Hepatol 1991; 13: 372–4.
19 Mu Y, Liu P, Du G, Du J, Wang G, Long A, *et al.* Action mechanism of Yi Guan Jian Decoction on CCl_4 induced cirrhosis in rats. J Ethnopharmacol 2009; 121: 35–42.
20 Peng JH, Hu YY, Cheng Y, Han C, Xu LL, Feng Q, *et al.* Effect of Jianpi Huoxue decoction on inflammatory cytokine secretion pathway in rat liver with lipopolysaccharide challenge. World J Gastroenterol 2008; 14: 1851–7.
21 Kleiner DE, Stetler-Stevenson WG. Quantitative zymography: detection of picogram quantities of gelatinases. Anal Biochem 1994; 218: 325–9.
22 Friedman SL. Hepatic stellate cells: protean, multifunctional, and enigmatic cells of the liver. Physiol Rev 2008; 88: 125–72.
23 Inagaki Y, Okazaki I. Emerging insights into transforming growth factor beta Smad signal in hepatic fibrogenesis. Gut 2007; 56: 284–92.
24 Jenkins SA, Grandison A, Baxter JN, Day DW, Taylor I, Shields R. A dimethylnitrosamine-induced model of cirrhosis and portal hypertension in the rat. J Hepatol 1985; 1: 489–99.
25 Li D, Friedman SL. Liver fibrogenesis and the role of hepatic stellate cells: new insights and prospects for therapy. J Gastroenterol Hepatol 1999; 14: 618–33.
26 Friedman SL. Mechanisms of disease: Mechanisms of hepatic fibrosis and therapeutic implications. Nat Clin Pract Gastroenterol Hepatol 2004; 1: 98–105.
27 Friedman SL. Mechanisms of hepatic fibrogenesis. Gastroenterology 2008; 134: 1655–69.
28 Bachem MG, Melchior R, Gressner AM. The role of thrombocytes in liver fibrogenesis: effects of platelet lysate and thrombocyte-derived growth factors on the mitogenic activity and glycosaminoglycan synthesis of cultured rat liver fat storing cells. J Clin Chem Clin Biochem 1989; 27: 555–65.
29 Bilzer M, Roggel F, Gerbes AL. Role of Kupffer cells in host defense and liver disease. Liver Int 2006; 26: 1175–86.
30 Ghiassi-Nejad Z, Friedman SL. Advances in antifibrotic therapy. Expert Rev Gastroenterol Hepatol 2008; 2: 803–16.
31 Gressner AM, Weiskirchen R. Modern pathogenetic concepts of liver fibrosis suggest stellate cells and TGF-beta as major players and therapeutic targets. J Cell Mol Med 2006; 10: 76–99.
32 Gressner AM. Cytokines and cellular crosstalk involved in the activation of fat-storing cells. J Hepatol 1995; 22: 28–36.
33 Bissell DM, Wang SS, Jarnagin WR, Roll FJ. Cell-specific expression of transforming growth factor-beta in rat liver. Evidence for autocrine regulation of hepatocyte proliferation. J Clin Invest 1995; 96: 447–55.
34 Shi Y, Massague J. Mechanisms of TGF-beta signaling from cell membrane to the nucleus. Cell 2003; 113: 685–700.
35 Piek E, Heldin CH, Ten Dijke P. Specificity, diversity, and regulation in TGF-beta superfamily signaling. FASEB J 1999; 13: 2105–24.